

NL 80A 0012



ASSOCIATIE EURATOM-FOM

FOM-INSTITUUT VOOR PLASMAFYSICA

RIJNHUIZEN - NIEUWEGEIN - NEDERLAND

**IDEAL MHD EQUILIBRIUM OF A
WEAKLY TOROIDAL PLASMA COLUMN
WITH ELONGATED CROSS-SECTION
PART II: FORCE-FREE FIELDS**

by

E.J.M. van Heesch and W. Schuurman

Rijnhuizen Report 80-124



**IDEAL MHD EQUILIBRIUM OF A WEAKLY
TOROIDAL PLASMA COLUMN WITH ELONGATED
CROSS-SECTION
PART II: FORCE-FREE FIELDS**

by

E.J.M. van Heesch and W. Schuurman

Rijnhuizen Report 80-124

C O N T E N T S

	page
Abstract	1
1. Introduction	2
2. Calculations force-free field	2
2.1 Introduction	2
2.2 Equilibrium equations	3
2.3 Solutions for B_z and j_z	5
2.4 First-order solution for ψ	6
2.5 Second-order solution for ψ	7
2.6 Properties of the first-order solution	7
2.7 Influence of second-order corrections	12
2.8 Calculation of q near the plasma surface	13
2.9 Combination of the results of first-order toroidal calculations and calculations of the force-free field	15
3. Discussion	16
4. References	16

IDEAL MHD EQUILIBRIUM OF A WEAKLY TOROIDAL PLASMA COLUMN
WITH ELONGATED CROSS-SECTION
PART II: FORCE-FREE FIELDS

by

E.J.M. van Heesch, W. Schuurman
Association Euratom-FOM
FOM-Instituut voor Plasmafysica
Rijnhuizen, Nieuwegein, The Netherlands

ABSTRACT

Solutions are obtained of the ideal MHD equations describing the equilibrium of a weakly toroidal plasma with an elliptic cross-section surrounded by a force-free magnetic field with constant ratio between current density and magnetic field strength. The force-free field parameter causes the stagnation points to recede along the major axis of the ellipse. Above a certain value of the force-free field parameter, stagnation points do not exist, so that the compression ratio of the plasma column is no longer limited. The analysis was carried out to first order in the force-free field parameter as well as to second order for an estimate of the error.

1. INTRODUCTION

In part I of the report the ideal MHD equilibrium was considered of a weakly toroidal plasma column of elliptical cross-section traversed by a homogeneous toroidal current and surrounded by vacuum.

In this second part we shall give the solution for a straight plasma column with elliptic cross-section surrounded by force-free currents: $\mu_0 \underline{j} = \alpha \underline{B}$. Taking α as a constant over the region around the plasma column we can solve the ideal MHD equations by a series expansion in the parameter α . After giving the solutions for the axial current and magnetic field, the flux equation is solved up to second order in α . The solutions enable us to investigate the influence of α on the geometry of the flux surfaces. The results are presented in analytical and graphical form. Since the first-order corrections for α and toroidicity are uncoupled, they can be combined to give an example of a weakly toroidal plasma surrounded by force-free currents.

2. CALCULATIONS FORCE-FREE FIELD

2.1 Introduction

The ideal MHD equations, describing the equilibrium of an elliptic plasma column surrounded by force-free currents (f.f.c.), will be solved by expansion in the f.f.c. parameter αa ; a is the minor half-axis of the plasma ellipse and α is defined by:

$$\mu_0 \underline{j} = \alpha \underline{B} , \quad (1)$$

where α is a constant.

Equation (1) represents the applied model for the f.f.c. region. In this low density plasma, currents are induced but the pressure gradient vanishes. In the plasma column we assume a homogeneous axial current density:

$$\underline{j} = j_0 \underline{z} . \quad (2)$$

The elliptic coordinate system we use is a normalization of the commonly known elliptic coordinates $x = c \sinh u \cos v$, $y = c \cosh u \sin v$:

$$\begin{aligned} x &= \frac{a}{\sinh u_0} \sinh u \cos v \\ y &= \frac{a}{\sinh u_0} \cosh u \sin v . \end{aligned} \quad (3)$$

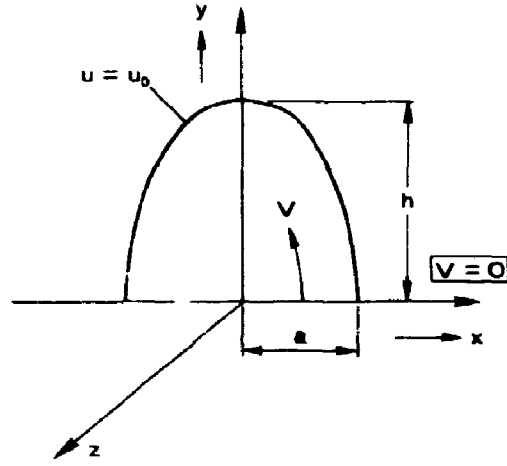


Fig. 1. The geometry and coordinate system.

Lines $u = \text{constant}$ form a set of confocal ellipses. The plasma column is bounded by the line $u = u_0$. The ellipticity of the column is:

$$e = \frac{h}{a} = \coth u_0, \quad (4)$$

where h is the major half-axis of the plasma ellipse.

In the following all physical quantities, here formally denoted by g , are expanded as follows:

$$g = g_0 + \alpha a g_1 + (\alpha a)^2 g_2. \quad (5)$$

g_0 , g_1 , g_2 are the zero-, first- and second-order parts of g respectively. g_0 represents the solution for a vacuum region surrounding the central plasma. This solution has been given by Gajewski¹⁾.

Furthermore, the indices v and f are used when necessary, to distinguish between the vacuum- and the f.f.c.-region respectively. The constant $\cosh 2u_0$ which appears frequently is denoted by s :

$$s = \cosh 2u_0. \quad (6)$$

2.2 Equilibrium equations

The metric coefficients of the coordinate system Eq. (3) to be inserted in the components of the vector-differential equations are:

$$h_u = h_v = \frac{1}{2} \sqrt{2} \frac{a}{\sinh u_0} (\cosh 2u + \cos 2v)^{1/2}, \quad (7)$$

$$h_z = 1. \quad (8)$$

Since $\frac{\partial}{\partial z} g = 0$, the divergence equation $\nabla \cdot \underline{B} = 0$ reduces to:

$$\frac{\partial}{\partial u} (h_u B_u) + \frac{\partial}{\partial v} (h_u B_v) = 0 . \quad (9)$$

With Eq. (1) the components of $\nabla \times \underline{B} = \mu_0 \underline{j}$ become:

$$\frac{\partial B_z}{\partial v} = \alpha h_u B_u , \quad (10)$$

$$\frac{\partial B_z}{\partial u} = -\alpha h_u B_v , \quad (11)$$

$$\frac{\partial}{\partial u} (h_u B_v) - \frac{\partial}{\partial v} (h_u B_u) = \begin{cases} \mu_0 j_0 h_u^2 ; u < u_0 \\ \alpha h_u^2 B_z ; u > u_0 . \end{cases} \quad (12)$$

$$\quad (13)$$

The only relevant components of $\nabla p = \underline{j} \times \underline{B}$ occur for $u < u_0$:

$$\frac{\partial p}{\partial u} = -j_0 h_u B_v \quad (14)$$

$$\frac{\partial p}{\partial v} = j_0 h_u B_u . \quad (15)$$

To solve Eqs. (12) and (13) we introduce a flux function $\psi(u,v)$ which satisfies Eq. (9):

$$\frac{\partial \psi}{\partial u} = h_u B_v , \quad (16)$$

$$\frac{\partial \psi}{\partial v} = -h_u B_u . \quad (17)$$

Inserting Eqs. (16) and (17) into Eq. (13) we arrive at the flux equation for the f.f.c. region:

$$\frac{\partial^2 \psi}{\partial u^2} + \frac{\partial^2 \psi}{\partial v^2} = \alpha h_u^2 B_z . \quad (18)$$

The addition of force-free currents to the outside region does not affect the boundary conditions for the flux equation of the plasma region. Consequently, the existing solution for this region (part I of this report, Refs. 1,2) remains valid and we have to solve only Eq. (18). The zero-order solution of this equation was given in part I of the report (Refs. 1,2).

The solutions referred to are:

$$\psi_0^p = \frac{\mu_0 j_0 a^2}{4s(s-1)} \{ s \cosh 2u - 1 + (\cosh 2u - s) \cos 2v \} \quad (19)$$

$$\psi_0^f = \frac{\mu_0 j_0 a^2}{4s(s-1)} \sinh 2u_0 \{ \sinh 2u_0 + 2s(u-u_0) + \sinh 2(u-u_0) \cos 2v \} . \quad (20)$$

The boundary conditions applied to obtain these solutions are:

$$\psi = 0 \quad \text{in } u = 0, \quad v = 0 , \quad (21)$$

$$\frac{\partial \psi}{\partial v} = 0 \quad \text{in } u = u_0 \text{ at both sides of the interface ,} \quad (22)$$

$$\left\{ \frac{\partial \psi}{\partial u} \right\}_{u_0} = 0 , \quad (23)$$

where $\{g\}_{u_0} = g^f - g^p$ in $u = u_0$ is the jump of g across the plasma boundary.

The first and second order parts of Eq. (18) are solved with the boundary conditions:

$$\psi_1(u_0) = \psi_2(u_0) = 0 , \quad (24)$$

$$\frac{\partial \psi_1}{\partial u}(u_0) = \frac{\partial \psi_2}{\partial u}(u_0) = 0 . \quad (25)$$

2.3 Solutions for B_z and j_z

Insertion of Eqs. (16) and (17) into Eqs. (10) and (11) leads to the following set of equations for B_z :

$$\frac{\partial B_z}{\partial v} = -\alpha \frac{\partial \psi}{\partial v} \quad (26)$$

$$\frac{\partial B_z}{\partial u} = -\alpha \frac{\partial \psi}{\partial u} , \quad (27)$$

with the solution:

$$B_z = B_0 - \alpha \psi . \quad (28)$$

B_0 is the axial field in vacuum. Equation (1) gives the solution for j_z :

$$j_z = \alpha B_0 - \alpha^2 \psi . \quad (29)$$

The final form of the flux equation in the ffc-region now becomes:

$$\frac{\partial^2 \psi}{\partial u^2} + \frac{\partial^2 \psi}{\partial v^2} = \alpha h_u^2 (B_0 - \alpha \psi) . \quad (30)$$

Separation of the solution of Eq. (30) in a solution by series expansion in α of the homogeneous equation and a particular solution:

$$\psi = B_0/\alpha \quad (31)$$

causes erroneous results after application of the boundary conditions. The ordering of the b.c.'s has to correspond to the ordering of ψ . We therefore start with the expansion of Eq. (30) by putting:

$$\psi = \psi_0 + (\alpha a)\psi_1 + (\alpha a)^2\psi_2 + (\text{H.O.}). \quad (32)$$

2.4 First-order solution for ψ

The equation for ψ_1 is the first-order part of Eq. (30):

$$\frac{\partial^2 \psi_1}{\partial u^2} + \frac{\partial^2 \psi_1}{\partial v^2} = \frac{\hbar^2}{a} B_0. \quad (33)$$

We look for solutions of the form:

$$\psi_1 = \sum_{n=0}^{\infty} F_n(u) \cos nv. \quad (34)$$

Substituting this into Eq. (33) we arrive at a set of differential equations for F_n which can be solved by standard techniques. The expressions obtained for F_n are:

$$F_0 = s_0 + c_0 u + \frac{aB_0}{4(s-1)} \cosh 2u, \quad (35)$$

$$F_2 = s_2 \sinh 2u + c_2 \cosh 2u - \frac{aB_0}{4(s-1)}, \quad (36)$$

$$F_n = s_n \sinh nu + c_n \cosh nu$$

for $n = 1; n = 3, 4, \dots$ (37)

The constants s_n and c_n are found by matching the solution to the boundary conditions Eqs. (24) and (25). The result reads:

$$s_0 = \frac{aB_0}{4(s-1)} (2u_0 \sinh 2u_0 - s), \quad (38)$$

$$c_0 = -\frac{aB_0}{2(s-1)} \sinh 2u_0, \quad (39)$$

$$s_2 = -\frac{aB_0}{4(s-1)} \sinh 2u_0, \quad (40)$$

$$c_2 = \frac{aB_0}{4(s-1)} s, \quad (41)$$

$$c_n = s_n = 0 \quad \text{for } n = 1; \quad n = 3, 4, \dots, \quad (42)$$

Summarizing the results we have:

$$\alpha a \psi_1 = \frac{\mu_0 j_0 a^2}{4(s-1)} \gamma \{ \cosh 2u - s - 2(u-u_0) \sinh 2u_0 + [\cosh 2(u-u_0) - 1] \cos 2v \}, \quad (43)$$

$$\text{with } \gamma = \frac{\alpha B_0}{\mu_0 j_0}. \quad (44)$$

2.5 Second-order solution for ψ

With the help of Eqs. (7) and (30) the second-order flux equation, becomes:

$$\frac{\partial^2 \psi_2}{\partial u^2} + \frac{\partial^2 \psi_2}{\partial v^2} = - \frac{1}{s-1} (\cosh 2u + \cos 2v) \psi_0(u,v). \quad (45)$$

Solutions of the form $\psi_2 = \sum_{n=0}^{\infty} F_n(u) \cos nv$ are derived in the same way as was done for the first-order flux function. After application of the boundary conditions (24) and (25) the resulting expression for ψ_2 reads:

$$\begin{aligned} \psi_2 = & - \frac{\mu_0 j_0 a^2 \tanh 2u_0}{16(s-1)^2} * \left\{ (u-u_0) (1+2s \cosh 2u) + s(\sinh 2u_0 - 2 \sinh 2u) \right. \\ & + \frac{1}{3} \{ \sinh 2(u-u_0) (s+\cosh 2u) + \sinh 2u - \sinh 2u_0 \} \cos 2v - 2s(u-u_0) \cos 2v + \\ & \left. + \frac{1}{6} \sinh 2(u-u_0) \{ \cosh 2(u-u_0) - 1 \} \cos 4v \right\}. \quad (46) \end{aligned}$$

2.6 Properties of the first-order solution

We investigate the influence of force-free currents on the shape of the flux surfaces around the plasma column. To obtain an impression of the values of the parameters involved, γ and α , we combine the first-order part of Eq. (29) with Eq. (44):

$$j_z = \gamma j_0, \quad (47)$$

$$\alpha = \gamma \frac{\mu_0 j_0}{B_0}. \quad (48)$$

For experimental conditions we have the order of magnitude of 1 for γ and α .

Gajewski¹⁾ showed that in vacuum the region of nested flux surfaces is bounded by a separatrix with two stagnation points (u_s, v_s) :

$$\begin{aligned} u_s &= 2 u_0, \\ v_s &= \pm \frac{1}{2} \pi. \end{aligned} \quad (49)$$

In these points B_u and B_v vanish. Confinement of the plasma within a closed conducting wall then severely limits the attainable compression ratio, see Part I, Ref. 2. The position of the stagnation points however, changes considerably by adding force-free currents. To calculate this effect we write ψ , up to first order:

$$\psi = f_0(u) + f_2(u) \cos 2v, \quad (50)$$

with:

$$f_0 = \left\{ \frac{\sinh^2 2u_0}{s} + 2(u-u_0)(1-\gamma) \sinh 2u_0 + \gamma(\cosh 2u - s) \right\} \frac{\mu_0 j_0 a^2}{4(s-1)}, \quad (51)$$

$$f_2 = \left\{ \frac{\sinh 2u_0}{s} \sinh 2(u-u_0) + \gamma(\cosh 2(u-u_0) - 1) \right\} \frac{\mu_0 j_0 a^2}{4(s-1)}. \quad (52)$$

The stagnation points are found by solving for u and v :

$$\frac{\partial \psi}{\partial v} = -2f_2 \sin 2v = 0, \quad (53)$$

$$\frac{\partial \psi}{\partial u} = f_0' + f_2' \cos 2v = 0. \quad (54)$$

Since f_2 remains positive for $u > u_0$, Eq. (53) has the solutions:

$$v_s = \pm \frac{1}{2} \pi; \quad v_s = 0; \quad v_s = \pi. \quad (55)$$

Because f_0' and f_2' also remain positive for $u > u_0$, Eq. (54) has solutions if:

$$\frac{1}{4} \pi < v_s < \frac{3}{4} \pi; \quad -\frac{3}{4} \pi < v_s < -\frac{1}{4} \pi. \quad (56)$$

Combination of Eqs. (55) and (56) yields the solution:

$$v_s = \pm \frac{1}{2} \pi. \quad (57)$$

After insertion of this result and Eqs. (51), (52) into Eq. (54) we obtain:

$$c_1 (\cosh 2u - 1) = c_2 \sinh 2u, \quad (58)$$

$$\text{with: } c_1 = s(1-\gamma) \sinh 2u_0 \text{ and } c_2 = (s-1)\{1+s(1-\gamma)\}. \quad (59)$$

We are interested only in real positive solutions $u = u_s$ of Eq. (58). They exist only if: $\text{sign}(c_1) = \text{sign}(c_2)$. The zeros of c_1 and c_2 are $\gamma = 1$ and $\gamma = 2e^2/e^2+1$ respectively, while c_1, c_2 are negative for large gammas. Hence, real positive solutions of Eq. (58) are restricted to:

$$\begin{aligned} \gamma < 1, \\ \gamma > \frac{2e^2}{e^2+1}. \end{aligned} \quad (60)$$

The solution of Eq. (58):

$$\cosh 2u_s = \frac{c_1^2 + c_2^2}{c_1^2 - c_2^2}, \quad (61)$$

has a singularity for $c_1 = c_2$ ($c_1 = -c_2$ is not allowed), i.e., for:

$$\gamma = \gamma_1 = \frac{e(e-1)}{e^2+1}. \quad (62)$$

For $\gamma_1 < \gamma \leq 1$ $\cosh 2u_s$ is negative and there are no real solutions u_s . Finally, Eq. (61) can be evaluated by substitution of Eqs. (59):

$$\cosh 2u_s = 2s^2 - 1 + 2\gamma s^2 \left\{ \frac{2(1-\gamma)s^2 + \gamma s + (\gamma-2)}{2\gamma(\gamma-i)s^2 + (1-2\gamma)s + 1} \right\}. \quad (63)$$

Next, we further restrict the possibility of stagnation points by demanding $u_s > u_0$. With the help of Eq. (63) we find that this condition holds only if

$$\gamma < \frac{3e^2+1}{2e^2+2}. \quad (64)$$

Summarizing Eqs. (60), (62) and (64) (see Fig. 2) we see that real stagnation points in the f.f.c. region only exist for

$$\gamma < \frac{e(e-1)}{e^2+1}. \quad (65)$$

In this case Eq. (63) gives the value of u_s .

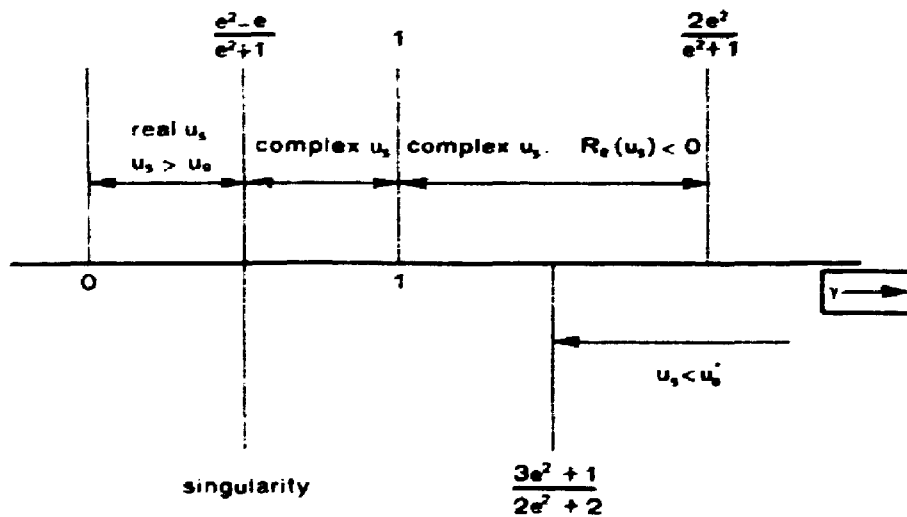


Fig. 2. One-dimensional graph along the γ -axis of regions of solutions of Eq. (58).

If stagnation points exist, the maximum of the radial compression ratio κ can be calculated by solving:

$$\psi(u_S, \frac{1}{2}\pi) = \psi(u_W, 0) \quad (66)$$

where κ is defined as:

$$\kappa = \frac{\sinh u_W}{\sinh u_O} \quad (67)$$

The numerical solution of Eq. (66) is depicted in Fig. 3. It shows clearly that, for example at a fixed ellipticity, κ_{\max} increases with γ until κ_{\max} becomes infinite. The relation between γ, e and the disappearance of the stagnation points (Eq. (65)) is plotted in Fig. 4.

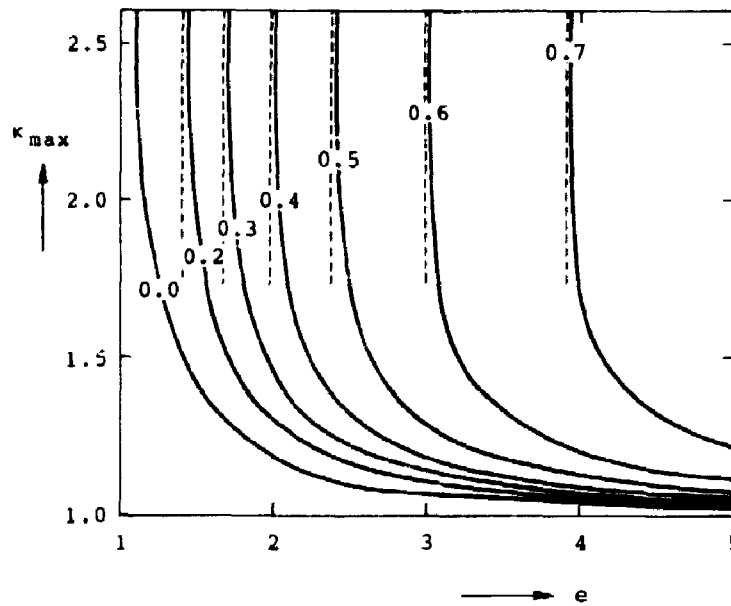


Fig. 3. The relation between the maximum of the compression ratio, κ_{\max} , and the ellipticity for several values of γ . Along the vertical lines κ_{\max} becomes infinite.

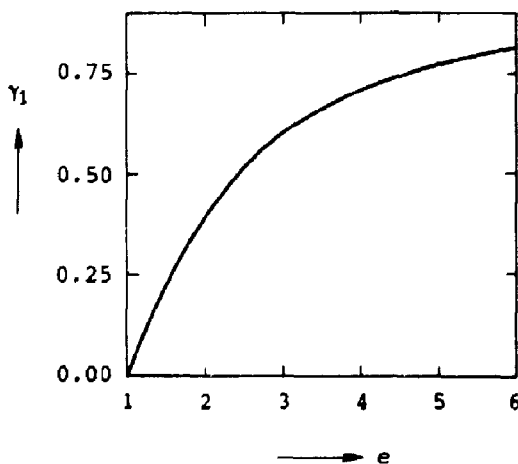


Fig. 4. The relation between γ and the ellipticity for which κ_{\max} becomes infinite.

Examples of the configuration of the flux surfaces for some values of e and γ are shown in Figs. 5 to 8.

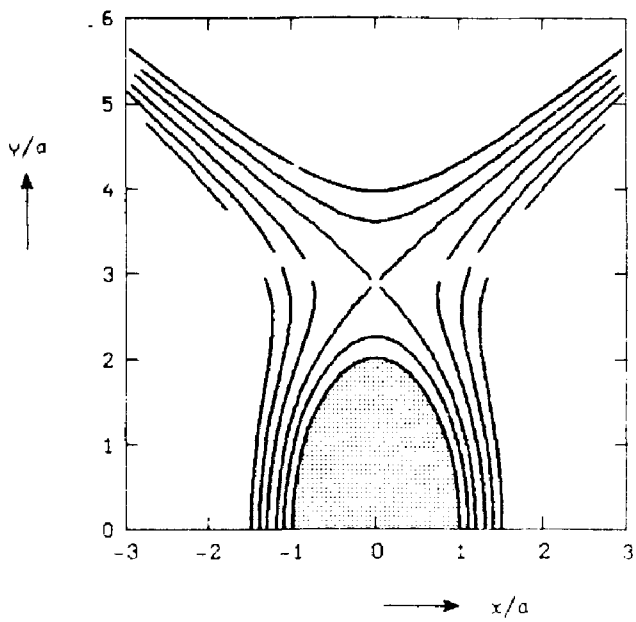


Fig. 5. Plot of flux surfaces for $e = 2, \gamma = 0$.

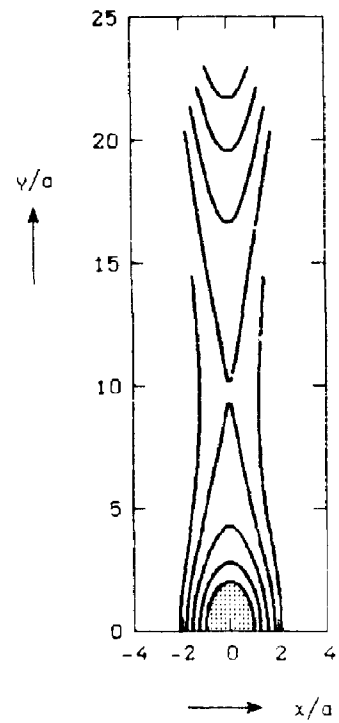


Fig. 6. Plot of flux surfaces for $e = 2, \gamma = 0.38$.

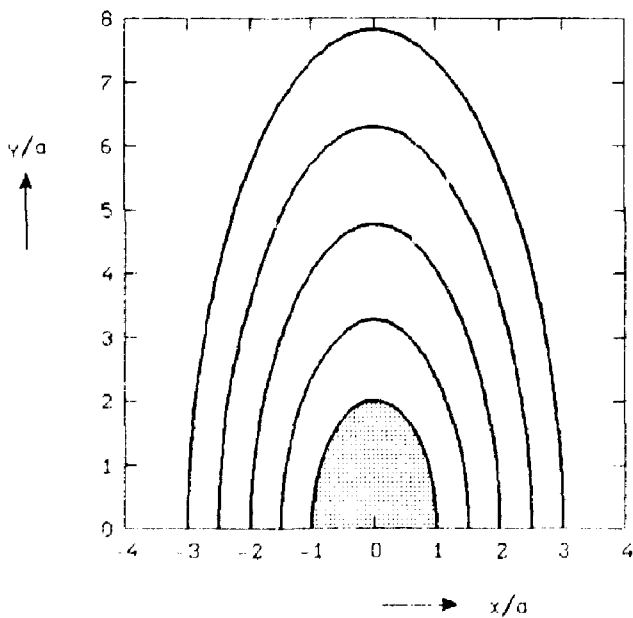


Fig. 7. Plot of flux surfaces for $e = 2, \gamma = 0.6$.

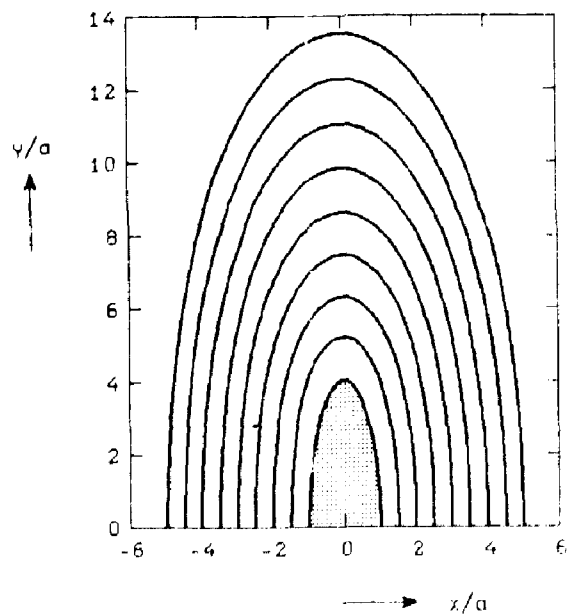


Fig. 8. Plot of flux surfaces for $e = 4, \gamma = 2.0$.

To obtain the plots we solved the equation for u:

$$\psi(u, v_j) = \psi(u_\kappa, 0) , \quad (68)$$

numerically, for an array of v_j values between 0 and π and for values of u_κ determined through relation (67) at chosen values of κ . Figures 4, 5 and 6 are plots for $e = 2$ and

$\gamma = 0$, vacuum , Fig. 5,

$\gamma = 0.38$, shifted stagnation point , Fig. 6,

$\gamma = 0.60$, disappeared stagnation point, Fig. 7.

Figure 8 is a plot for $e = 4$, $\gamma = 2.0$. These values correspond to parameters measured in the SP IV experiment³⁾. In this experiment the plasma is surrounded by a closed copper shell which, however, is not elliptic but shaped like a racetrack. The copper shell coincides with a flux surface and stagnation points cannot exist unless current reversal takes place. The implosion which heats and creates the plasma, always yields values of κ around 4 and $e \geq 4$. A rough estimate then shows that γ must remain greater than 0.7 in order to have an equilibrium, consistent with the model described in this report, that excludes the existence of stagnation points.

2.7 Influence of second-order corrections

Making use of Eqs. (20), (43) and (46) we calculate the relative second-order correction on the value of ψ :

$$\left\{ \frac{(\alpha a)^2 \psi_2}{\psi_0 + \alpha a \psi_1} \right\} , \quad (69)$$

for the examples in Figs. 5 to 8. The following table contains the approximate maxima of Eq. (69), found along a certain flux line labeled by column 3. The value of αa is taken equal to 0.1.

e	γ	κ	<u>max. rel. correction</u>
2	0.38	κ_{\max}	0.07
2	0.60	2	0.007
2	0.60	3	0.008
4	2.0	2	0.002
4	2.0	3	0.004
4	2.0	4	0.01
4	2.0	5	0.03

We see that the second-order correction remains surprisingly low for flux surfaces of interest.

2.8 Calculation of q near plasma surface

The equations describing a magnetic field line are:

$$\frac{h_u}{B_v} dv = \frac{h_u}{B_u} du = \frac{h_\phi}{B_\phi} d\phi . \quad (70)$$

From this it follows that for this field line:

$$d\phi = \frac{B_\phi h_u}{B_v h_\phi} dv . \quad (71)$$

We have introduced the metric coefficient h_ϕ since we compute q for a torus. In a toroidal system $B_v h_\phi$ can be expressed in terms of ψ by the toroidal analogue of Eq. (16) (see part I, Ref. 2):

$$B_v h_\phi = \frac{R}{h_u} \frac{\partial \psi}{\partial u} . \quad (72)$$

The pitch q to be calculated is the fraction of toroidal angle traversed by a magnetic field line after one poloidal turn:

$$q = \frac{1}{2\pi} \int_{v=0}^{v=2\pi} d\phi(v) . \quad (73)$$

Equations (71), (72) inserted into Eq. (73) yield the general expression for q :

$$q = \frac{1}{\pi R} \int_0^\pi \left. \frac{B_\phi h_u^2}{\partial \psi / \partial u} \right]_{\psi = \text{constant}} dv . \quad (74)$$

The evaluation of this expression will be carried out for the case of the straight plasma ellipse with force-free currents, an artificial R and notation $\phi \rightarrow z$. The expression for $B_\phi = B_z$, Eq. (28), does not depend on v on a flux surface, and can therefore be taken out of the integral of Eq. (74). Near the plasma surface the resulting part of the integrand of Eq. (74) is evaluated analytically by a first-order expansion of u around u_0 :

$$u = u_0 + \epsilon , \quad (75)$$

Expanding the total flux, Eqs. (20) and (43) we find accordingly:

$$\psi = \psi_p \left(1 + 2\epsilon \frac{s + \cos 2v}{\sqrt{s^2 - 1}} \right) , \quad (76)$$

$$\text{where } \psi_p = u_0 j_0 a^2 \frac{s+1}{4s} . \quad (77)$$

ψ_p is the value of ψ at $u = u_0$.

Equation (76) is the relation between ϵ and ψ which we need in the following. The variable $h_u^2 \Big|_{\psi=\text{constant}}$, which appears in Eq. (74) is expanded with the help of Eq. (7):

$$h_u^2 \Big|_{\psi=\text{constant}} = \frac{a^2}{s-1} (\cos 2v + s + 2\epsilon \sqrt{s^2-1}) . \quad (78)$$

To evaluate $\partial\psi/\partial u$ we expand as follows:

$$\frac{\partial\psi}{\partial u} = \frac{\partial\psi}{\partial u} (u_0) + \epsilon \frac{\partial^2\psi}{\partial u^2} (u_0) . \quad (79)$$

With the expression for ψ Eqs. (20) and (43) it follows that:

$$\frac{\partial\psi}{\partial u} \Big|_{\psi=\text{constant}} = 2\psi_p \frac{s + \cos 2v}{\sqrt{s^2-1}} \left(1 + 2\epsilon \frac{\gamma s}{\sqrt{s^2-1}} \right) . \quad (80)$$

We insert the results Eqs. (78) and (80) into Eq. (74), make use of Eq. (28), and retain only first-order terms in ϵ . After replacement of ϵ by means of Eq. (76), the following expression for q results:

$$q = a^2 \frac{B_0^{-\alpha\psi}}{2\pi R \psi_p} e \left[\pi + \left(\frac{\psi}{\psi_p} - 1 \right) \left\{ (s^2-1) \int_0^\pi \frac{dv}{(\cos 2v+s)^2} - \gamma s \int_0^\pi \frac{dv}{\cos 2v+s} \right\} \right] . \quad (81)$$

The integrals in Eq. (81) can be calculated analytically and after replacement of s by its expression in e the result becomes:

$$q = \frac{a^2 e}{2R} \frac{B_0^{-\alpha\psi}}{\psi_p} \left\{ 1 + \left(\frac{\psi}{\psi_p} - 1 \right) \frac{e^2+1}{4e^2} (2e - \gamma(e^2-1)) \right\} . \quad (82)$$

This expression represents the relation $q = q(\psi)$ near the plasma surface. To obtain an impression of the q -profile we can, for example, examine $\partial q/\partial\psi$. Up to first order in α this derivative is at the plasma surface:

$$\frac{1}{q} \frac{\partial q}{\partial\psi} (u_0) = - \frac{\alpha}{B_0} + \frac{1}{\psi_p} \frac{e^2+1}{4e^2} (2e - \gamma(e^2-1)) . \quad (83)$$

The sign of $\frac{\partial q}{\partial\psi} (u_0)$ depends on the parameters α , B_0 , j_0 , a and e . In ideal screw-pinch experiments the q -profile is flat and, consequently,

$\frac{\partial g}{\partial \psi}(u_0) = 0$. For this latter condition to be fulfilled, Eq. (83) gives by making use of Eqs. (44) and (77):

$$(\alpha a)^2 = \frac{1}{2} \gamma \left(\frac{e^2+1}{e^2} \right)^2 (2e - \gamma(e^2-1)) . \quad (84)$$

Equation (84) has no solutions if the right-hand side is negative, i.e.:

$$\gamma > \frac{2e}{e^2-1} . \quad (85)$$

Combining this with the result obtained in Eq. (65) we find that in our model equilibria without stagnation points having $\frac{\partial g}{\partial \psi}(u_0) \geq 0$, can only exist for $e \leq 3.383$.

2.2 Combination of the results of first-order toroidal calculations and calculations of the force-free field

We can combine Eq. (51) of part I (Ref. 2) with Eqs. (20), (43) of this report to obtain an expression for the flux function in a model which contains a first-order toroidal correction and a force-free field surrounding the plasma column. The force-free field is described to first order in the force-free current parameter α . Figure 9 gives a plot of the resulting flux surfaces for $R/a = 16$, $e = 4$, $\beta_p = 8$, $\gamma = 1$, $\alpha a = 0.1$.

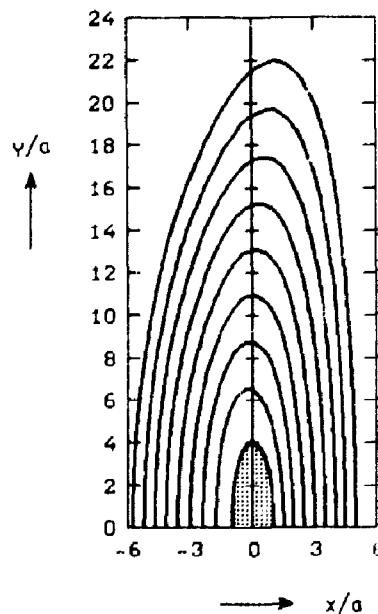


Fig. 9. Plot of flux surfaces of a toroidal plasma column surrounded by a constant α force-free field.

3. DISCUSSION

We have determined analytically elliptic equilibria of a slightly toroidal plasma column (Part I) and of a straight column surrounded by force-free currents (Part II). In Part I it was shown that an increasing ellipticity reduces the toroidal shift. The possibility of confining the elliptic plasma within a closed conducting wall is limited severely because, as a result of the geometry, a separatrix develops close to the plasma column. We can overcome this difficulty by allowing force-free currents to be induced in a dilute plasma around the central column. The calculation in Part II shows that the separatrix moves away from the central column if the force-free current parameter γ is increased. Above a certain limit of this parameter the separatrix disappears, thus allowing a closed conducting wall to surround the plasma at any realistic distance. The profile of the pitch of the magnetic field lines, which is flat in screw pinches, could only be calculated analytically in the region close to the plasma boundary. Results indicate that at high values of γ , $\frac{dg}{d\psi}(u_0)$ becomes negative.

4. REFERENCES

1. Gajewski, R., Phys. Fluids 15 (1972) 70.
2. Schuurman, W., van Heesch, E.J.M., Rijnhuizen Report 79-121 (1979).
3. Van Heesch, E.J.M. et al., Proc. 8th Eur. Conf. on Contr. Fusion and Plasma Phys., Prague (1977) Vol. I, p. 73.

This work was performed as part of the research programme of the association agreement of Euratom and the "Stichting voor Fundamenteel Onderzoek der Materie" (FOM) with financial support from the "Nederlandse Organisatie voor Zuiver-Wetenschappelijk Onderzoek" (ZWO) and Euratom.